One-loop calculations in the chirality-flow formalism

Andrew Lifson and Malin Sjödahl
Department of Physics, Lund University, Box 118, 221 00 Lund, Sweden

Simon Plätzer
Institute of Physics, NAWI Graz, University of Graz, Universitätsplatz 5, A-8010 Graz, Austria
and Particle Physics, Faculty of Physics, University of Vienna, Boltzmanngasse 5, A-1090 Wien, Austria

In a few recent papers we introduced the chirality-flow formalism, which builds on the spinor-helicity formalism, but incorporates the Fierz identity into the Feynman rules. Calculations at tree level are thereby trivial, often to the extent that it is possible to immediately write down a tree-level Feynman diagram in terms of spinor inner products. This simplification persists in tree-level computer implementations, giving very sizable speedups. In the present paper, we argue that there is also a significant simplification of the Lorentz structure at the one-loop level when using the four-dimensional formulation of the four-dimensional helicity scheme. As at tree level, the gauge reference vector for external gauge bosons, and the simplified Lorentz structure lead to significant shortening of the calculations. Additionally, we find that the possible terms in a tensor decomposition of loop integrals are highly constrained, and therefore the tensor reduction procedure is simplified.

I. INTRODUCTION

Recently, we introduced the chirality-flow formalism [1–4], which builds on the spinor-helicity formalism [5–23], and relies on splitting the Lorentz algebra into left- and right-chiral parts. As for the spinor-helicity formalism, all objects, in particular polarization vectors, are rewritten in terms of massless spinors, but the chirality-flow method takes the simplification one step further by recasting everything into diagrammatic "flows," i.e., contractions of spinors.

This allows for rewriting Feynman rules and diagrams directly in terms of these flows, and results in amplitudes that may be directly expressed in terms of spinor inner products, i.e., the only Lorentz invariant quantities at hand [1,2].

For tree-level calculations, the chirality-flow formalism leads to significant simplifications [1,2], to the extent that it is often possible to immediately write down the amplitude corresponding to a Feynman diagram. On top of this, reference vectors for external gauge bosons or spin directions can be chosen in such a way that many Feynman diagrams simplify or vanish. This—as well as the simplified

algebra—has led to a significant speedup for a tree-level QED test implementation in MadGraph5_aMC@NLO [3], for high multiplicities exceeding a factor 10 for $e^+e^- \to n\gamma$. Ongoing work shows a sizable speedup also for the QCD Lorentz structure. Besides their promising use in fixed-order tree-level calculations, we have also demonstrated [4] that chirality flow can be used to directly decompose amplitudes in terms of the available group and spinor structures and therefore is of utmost importance to provide reliable input to resummation approaches at the amplitude level [24–27].

Moving beyond tree level, it is imperative to use a consistent regularization scheme, which requires a careful treatment of chirality and γ^5 [28–44]. A comprehensive summary of different regularization methods can be found in [45,46]. In conventional dimensional regularization (CDR) [28,29,47], all objects are regularized in d dimensions, which (at least naively) would destroy many of the simplifications brought about by chirality flow. While in the long term we aim at a full treatment of chirality flow in CDR (such as to use chirality flow to extract ϵ-dependent quantities in tree-level calculations), in the present paper we instead exploit a (partially) four-dimensional regularization scheme, the 4D formulation (FDF) [48] of the 4D helicity scheme (FDH)[1] [51,52], in order to retain the significant simplifications which chirality flow draws from using charge conjugations, Fierz and Schouten identities. In

---

[1]The equivalence of FDH (and therefore FDF) to CDR is shown in [49,50].

FDF, loop numerators are written as purely four-dimensional objects together with some additional Lorentz scalars, while the loop momenta and integrals are in d dimensions. This implies that the algebraic manipulations implemented for tree-level calculations in four dimensions [1,2] can be retained, and Feynman diagrams are therefore easily "flow-able"—as in tree-level calculations.[2] After simplifying the Lorentz algebra the integrals are in d dimensions, implying that we can use all of the standard properties and results of dimensionally regularized integrals.

The rest of this paper is organized as follows. In Sec. II, we give a brief introduction to chirality flow and how it is used in Feynman-diagram-based amplitude calculations. Then, the 4D formulation of the 4D helicity scheme is introduced in Sec. III. In Sec. IV, we illustrate with a few examples how to perform one-loop calculations in chirality flow, describing how chirality flow simplifies the Lorentz algebra and tensor reduction. Finally, we conclude in Sec. V.

II. INTRODUCTION TO CHIRALITY FLOW

In this section, we give a brief introduction to the chirality-flow formalism, and exemplify how spinors, propagators, and vertices are defined. A complete list of Standard Model external wave functions, vertices, and propagators can be found in [2], whereas all structures needed for this paper are contained either in the main text or in the Appendix. For details of conventions, we refer the reader to [1].

The basic building blocks of the chirality-flow formalism are the left- and right-chiral spinors, which we represent graphically in terms of dotted and undotted lines respectively [1],

$$\langle i| = \quad i \quad , \quad [i| = \quad i \quad , \tag{1}$$
$$|j\rangle = \quad j \quad , \quad |j] = \quad j \quad ,$$

with $\langle i| = \langle p_i|$ etc. We represent contractions of these spinors with "flows"

$$\langle ij\rangle \equiv \epsilon^{\alpha\beta}\lambda_{i,\beta}\lambda_{j,\alpha} = \quad i \longrightarrow j \quad ,$$
$$[ij] \equiv \epsilon_{\dot\alpha\dot\beta}\tilde\lambda_i^{\dot\beta}\tilde\lambda_j^{\dot\alpha} = \quad i \cdots\cdots\rightarrow\cdots\cdots j \quad , \tag{2}$$

where (up to a phase) $\langle ij\rangle \sim [ij] \sim \sqrt{2p_i \cdot p_j}$, and where the antisymmetry of the spinor inner product is obvious. We read chirality-flow lines along the chirality-flow arrow, and, because the inner product is antisymmetric, swapping the chirality-flow arrow direction induces a minus sign.

All particles and momenta are then written as (a combination of) massless spinors.[3] For example, massless polarization vectors are given by

$$\epsilon_L(p_i, r) = \frac{1}{\langle ri\rangle} \quad \begin{matrix} i \\ r \end{matrix} \quad \text{or} \quad \frac{1}{\langle ri\rangle} \quad \begin{matrix} i \\ r \end{matrix} \quad ,$$
$$\epsilon_R(p_i, r) = \frac{1}{[ir]} \quad \begin{matrix} r \\ i \end{matrix} \quad \text{or} \quad \frac{1}{[ir]} \quad \begin{matrix} r \\ i \end{matrix} \quad , \tag{3}$$

where, similar to chiral spinors, we label the polarization vectors L/R for convenience,[4] with $\epsilon_L(p_i, r)$ denoting a negative-helicity incoming or positive-helicity outgoing photon of momentum p_i, and $\epsilon_R(p_i, r)$ denoting a positive-helicity incoming or negative-helicity outgoing photon. Here, r is an arbitrary (massless) reference vector with $r \cdot p_i \neq 0$, and either set of opposing arrow directions may be used as long as it matches the rest of the diagram [1].

To describe massive particles and momenta, a massive momentum p with $p^2 = m^2 \neq 0$ is decomposed into a sum of massless momenta $p^\flat$ and q as

$$p^\mu = p^{\flat,\mu} + \alpha q^\mu, \qquad (p^\flat)^2 = q^2 = 0,$$
$$p^2 = m^2, \qquad \alpha = \frac{m^2}{2p^\flat \cdot q} = \frac{m^2}{2p \cdot q}, \tag{4}$$

with, for example, an incoming spinor with spin along the axis $s^\mu = (p^\mu - 2\alpha q^\mu)/m$ given by[5] [2]

$$u^+(p) = \begin{pmatrix} \frac{m}{[p^\flat q]} \quad \cdots\cdots\rightarrow\cdots\cdots q \\ \quad \longrightarrow p^\flat \end{pmatrix} . \tag{5}$$

While it is natural in chirality flow to measure spin along any direction, we can of course also measure it along the direction of motion, in which case we choose $\alpha = 1$, $q^\mu = p_b^\mu$ and $p^{\flat,\mu} = p_f^\mu$, with $\vec{p}_f$ pointing in the same direction as $\vec{p}$ and $\vec{p}_b$ pointing in the opposite direction, i.e.,

$$p_f^\mu = \frac{p^0 + |\vec{p}|}{2}(1, \hat{p}), \quad p_b^\mu = \frac{p^0 - |\vec{p}|}{2}(1, -\hat{p}), \tag{6}$$

such that the three-vector of the spin $s^\mu = \frac{1}{m}(p_f^\mu - p_b^\mu) = \frac{1}{m}(|\vec{p}|, p^0\hat{p})$, is directed along the motion, giving the helicity basis,

---

[2]It is likely also possible to use chirality flow in other four-dimensional regularization schemes such as [53–70], but we do not explore this here.

[3]Scalar particles have no Lorentz structure and therefore no flow representation.

[4]The L/R label of a photon is given by the chirality of the spinor in its numerator containing its momentum.

[5]We use the chiral basis for the Dirac γ matrices.

$$u^+(p) = \begin{pmatrix} \frac{m}{[p_f p_b]} \ \text{} \\ \text{} \end{pmatrix}$$

$$\xrightarrow{m \to 0} \begin{pmatrix} \ 0 \\ \text{} \end{pmatrix}. \tag{7}$$

Vertices and propagators are also naturally described using chirality flow. For example, the QED vertex can be translated to

$$\text{}^\mu = ieQ_f \gamma^\mu = ieQ_f \begin{pmatrix} 0 & \sqrt{2}\tau^{\mu,\dot\alpha\beta} \\ \sqrt{2}\bar\tau^\mu_{\alpha\dot\beta} & 0 \end{pmatrix}$$

$$= ieQ_f\sqrt{2}\begin{pmatrix} 0 & \text{} \\ \text{} & 0 \end{pmatrix}, \tag{8}$$

where our use of the chiral basis is made explicit, and where we introduce our (differently normalized) Pauli matrices $\tau^\mu \equiv \sigma^\mu/\sqrt{2}$ and $\bar\tau^\mu \equiv \bar\sigma^\mu/\sqrt{2}$, to avoid factors of 2 in the Fierz identity.

The propagator for a massless gauge boson in the Feynman gauge contains the chirality-flow rule for the metric, which is a double line with arrows opposing,

$$\mu \sim\!\!\!\xrightarrow{p}\!\!\!\sim \nu = -i\frac{g_{\mu\nu}}{p^2}$$

$$\to -\frac{i}{p^2} \text{} \quad \text{or} \quad -\frac{i}{p^2} \text{}, \tag{9}$$

while the fermion propagator in the flow picture is

$$\xleftarrow{p} = \frac{i}{p^2-m^2}\begin{pmatrix} m\delta^{\dot\alpha}{}_{\dot\beta} & \sqrt{2}p^{\dot\alpha\beta} \\ \sqrt{2}\bar p_{\alpha\dot\beta} & m\delta_\alpha{}^\beta \end{pmatrix}$$

$$= \frac{i}{p^2-m^2}\begin{pmatrix} m\text{} & \text{} \\ \text{} & m\text{} \end{pmatrix}, \tag{10}$$

where we have introduced a graphical "momentum-dot" notation for momenta slashed with σ or $\bar\sigma$. Note that any momentum in the Feynman rules will be translated to this momentum dot in the chirality-flow rules using

$$p^\mu \to \frac{1}{\sqrt{2}} \text{} \quad, \quad \text{or} \quad p^\mu \to \frac{1}{\sqrt{2}} \text{} , \tag{11}$$

where, like with the polarization vectors in Eq. (3), either arrow direction in Eqs. (9) and (11) is allowed as long as it matches the rest of the diagram [1].

Using these rules, it is easy to immediately write down the values of Feynman diagrams, for example, in massless QED,

$$= \underbrace{(\sqrt{2}ei)^8}_{\text{vertices}} \underbrace{\frac{(-i)^3}{s_{12}\,s_{34}\,s_{78910}}}_{\text{photon propagators}} \underbrace{\frac{(i)^4}{s_{125}\,s_{346}\,s_{8910}\,s_{910}}}_{\text{fermion propagators}}$$

$$\times \underbrace{\frac{1}{[8\,r_8][9\,r_9]}}_{\text{polarization vectors}} [15]\langle 64\rangle[10\,r_9]\left(\underbrace{\langle 99\rangle}_{0}[9r_8] + \langle 9\,10\rangle[10\,r_8]\right)$$

$$\times \left(\underbrace{[33]}_{0}\langle 37\rangle + [34]\langle 47\rangle + [36]\langle 67\rangle\right)$$

$$\times \left(-\langle 89\rangle[91]\langle 12\rangle - \langle 89\rangle[95]\langle 52\rangle\right.$$

$$\left. -\langle 8\,10\rangle[10\,1]\langle 12\rangle - \langle 8\,10\rangle[10\,5]\langle 52\rangle\right), \tag{12}$$

where we have superimposed a chirality-flow diagram onto a ten-point Feynman diagram. For massless QED and QCD, any chirality-flow arrow direction which has opposing arrows for bosons and which flows through momentum dots is equivalent [1]. If masses or scalar particles are involved, some care is needed to set consistent arrow directions [2].

Finally, we also note that diagrams can be made to vanish by appropriately choosing the reference vectors of our polarization vectors and massive spinors. For example, the above diagram vanishes if we pick $r_9 = p_{10}$.

In this paper, we argue that much of the simplification from chirality flow can be retained at the one-loop level. In particular a good choice of gauge boson reference vector is transparently shown to cancel many terms. More generally, spinor contractions, the Weyl equation, the Fierz identity, and other identities simplify the algebra and demonstrate that we can fully exploit a graphical algorithm beyond tree

level. For example, we may simplify the algebra of the electron self-energy in Feynman gauge as

$$\sim \qquad \overset{p+l}{\underset{\bullet}{\text{------}}} \, , \qquad (13)$$

where we defer a discussion on the arrow direction until Sec. IV. The diagrammatic identity above is of course simple, but we will demonstrate that similar diagrammatic decompositions can be used together with methods of decomposing tensor integrals, and thereby significantly simplify calculations.

III. FDF

In this section we summarize the FDF formalism. This formalism was created in 2014 with the aim of providing a truly four-dimensional numerator algebra for loop integrals. It has also been used in the context of color-kinematics duality [71,72], while some example calculations in FDF can be found in [42,45]. Since the chirality-flow formalism makes use of explicitly four-dimensional relations, the FDF method is easily converted into a flow formalism (though we expect that a similar flow formalism holds in CDR).

In FDF we have five vector spaces, the standard Minkowski space $S_{[4]}$ with four integer dimensions, and the infinite-dimensional spaces $QS_{[d]}$, $QS_{[d_s]}$, $QS_{[-2\epsilon]}$, $QS_{[n_\epsilon]}$, and $QS_{[n_\epsilon-2\epsilon]}$, which satisfy [48]

$$S_{[4]} \subset QS_{[d]} \subset QS_{[d_s]}, \qquad QS_{[d]} = S_{[4]} \oplus QS_{[-2\epsilon]},$$
$$QS_{[n_\epsilon-2\epsilon]} = QS_{[-2\epsilon]} \oplus QS_{[n_\epsilon]}, \qquad QS_{[d_s]} = QS_{[d]} \oplus QS_{[n_\epsilon]},$$
$$(14)$$

where $QS_{[d]}$ is the vector space of CDR, $QS_{[d_s]}$ with $d_s = 4$ is the vector space of FDH and FDF, and we follow the notation of [45,73]. Since the subspaces in Eq. (14) are orthogonal, we can split up vectors and tensors as, e.g.,

$$\gamma^\mu_{[d_s]} = \gamma^\mu_{[4]} + \gamma^\mu_{[n_\epsilon-2\epsilon]}, \qquad g^{\mu\nu}_{[d_s]} = g^{\mu\nu}_{[4]} + g^{\mu\nu}_{[n_\epsilon-2\epsilon]}, \qquad (15)$$

where the subscript in square brackets gives the vector space of the object. The metric is used to project onto the different subspaces, for example,

$$g^{\mu\nu}_{[d_s]} g_{\nu\rho[4]} = \delta^\mu_{\rho[4]}, \qquad g^{\mu\nu}_{[d_s]} g_{\nu\rho[d]} = \delta^\mu_{\rho[d]}, \qquad (16)$$

while the trace of the metric is given by the dimension of its (sub)space, and the Dirac gamma matrices have their usual anticommutation relations

$$(g_{[\text{dim}]})^\mu_{\ \mu} = dim, \qquad \{\gamma^\mu_{[\text{dim}]}, \gamma^\nu_{[\text{dim}]}\} = 2g^{\mu\nu}_{[\text{dim}]}. \qquad (17)$$

The main starting point of FDF is to rewrite $QS_{[d_s]}$ as

$$QS_{[d_s]} = S_{[4]} \oplus QS_{[-2\epsilon]} \oplus QS_{[n_\epsilon]} = S_{[4]} \oplus QS_{[n_\epsilon-2\epsilon]}, \qquad (18)$$

that is, as the purely 4D Minkowski space plus an extra space $QS_{[n_\epsilon-2\epsilon]}$ which can be represented by 4D objects multiplying a new algebra called the -2ϵ selection rules (-2ϵ-SRs). The -2ϵ-SRs are defined using the following replacements,

$$g^{\mu\nu}_{[n_\epsilon-2\epsilon]} \to G^{MN}, \qquad l^\mu_{[-2\epsilon]} \to i\mu Q^M, \qquad \gamma^\mu_{[n_\epsilon-2\epsilon]} \to \gamma^5 \Gamma^M, \qquad (19)$$

together with the following algebra,

$$G^{MN} G^{NP} = G^{MP}, \qquad G^{MM} = 0, \qquad G^{MN} = G^{NM},$$
$$\Gamma^M G^{MN} = \Gamma^M, \qquad \Gamma^M \Gamma^M = 0, \qquad Q^M \Gamma^M = 1,$$
$$Q^M G^{MN} = Q^M, \qquad Q^M Q^M = 1, \qquad \{\Gamma^M, \Gamma^N\} = 2G^{MN}.$$
$$(20)$$

In any given Feynman diagram the -2ϵ-SRs can be precalculated, and contribute an overall multiplicative factor of 0 or ± 1 to the diagram.

In the Feynman rules of FDF, the -2ϵ-SRs imply that fermion propagators within loops are rewritten to contain only 4D terms and a new mass[6] μ [48],

$$\overset{p}{\longleftarrow} \sim \, l\!\!\!/_{[d_s]} + m = l\!\!\!/_{[4]} + i\mu\gamma^5 + m$$

$$= \left((m - i\mu) \overset{}{\underset{l}{\text{-----}\blacktriangleright\text{-----}}} \quad \overset{l}{\underset{}{\text{--}\blacktriangleright\text{--}\bullet\text{--}}} \right),$$
$$\qquad \qquad \overset{}{\underset{l}{\text{--}\blacktriangleright\text{--}\bullet\text{--}}} \quad (m + i\mu) \overset{}{\underset{}{\longrightarrow}} \right), \qquad (21)$$

and that vector boson propagators are split into two pieces, with numerator structure

$$\mu \sim\!\!\!\!\overset{p}{\sim\!\!\!\sim}\!\!\!\!\sim \nu \, \sim -ig^{\mu\nu}_{[d_s]} = -ig^{\mu\nu}_{[4]} - iG^{MN}$$
$$= -i \, \overset{}{\underset{}{\text{---------}}} \, - iG^{MN}, \qquad (22)$$

in Feynman gauge. Here, the first term is the usual 4D propagator with suppressed chirality-flow arrows (recall that these arrows should be opposing; see Sec. II), and the

---

[6]This mass should not be confused with the 't Hooft mass, but signifies the extra-dimensional part of the loop momentum; see Eq. (24).

second is called an FDF scalar and has trivial Lorentz structure.[7]

To build the correct Feynman diagrams with FDF, we must use the FDF Feynman rules, which can be found in [48]. These rules include new terms not present at tree level in chirality flow. However, these new terms are all either Lorentz scalars and therefore have no flow representation, or contain additional momenta which have the chirality-flow representation in Eq. (11), the metric which has the chirality-flow representation in Eq. (9), or γ^5 which only affects the overall sign of a chirality-flow graph. Therefore, we do not show them explicitly here.

All loop integrals $I^d_{i_1...i_k}[N^{\mu_1...\mu_n}]$ in FDF, and therefore all loop momenta $l^\mu_{[d]}$, are in d dimensions. The loop integral is defined in the usual way:

$$I^d_{i_1...i_k}[N^{\mu_1...\mu_n}] \equiv \int \frac{d^d l_{[d]}}{(2\pi)^d} \frac{N^{\mu_1...\mu_n}}{D_{i_1}...D_{i_k}}, \qquad (23)$$

for $N^{\mu_1...\mu_n}$ some numerator which may be a scalar, vector, or general tensor in Lorentz space, and D_i a propagator momentum of the usual form $p^2_{[d]} - m^2$. When squaring a loop momentum we use the -2ϵ-SRs, Eqs. (19) and (20), to obtain

$$l^\mu_{[d]} = l^\mu_{[4]} + l^\mu_{[-2\epsilon]}, \qquad l^2_{[d]} = l^2_{[4]} + l^2_{[-2\epsilon]} = l^2_{[4]} - \mu^2, \qquad (24)$$

where we identify the spacelike mass $l^2_{[-2\epsilon]} = -\mu^2$. A defining feature of FDF is that only even powers of μ are allowed to contribute to the amplitude. Integrals involving μ^2 are reduced to integrals without μ^2 using [74]

$$I^d_{i_1...i_k}[(\mu^2)^r] = (2\pi)^r I^{d+2r}_{i_1...i_k}[1] \prod_{j=0}^{r-1}(d - 4 - 2j). \qquad (25)$$

The above identity is essentially related to dimensional shift relations originating from powers of the loop momentum in the numerator, as, e.g., also employed in the decomposition of tensor integrals [75].

From the above, we see that all of the Lorentz algebra is done in four dimensions and is easily "flowable," while all loop integrals are conveniently performed in d dimensions.

IV. FLOWING LOOPS

In this section we show how to turn the FDF formalism into a chirality-flow formalism. To understand how this works, it is useful to first go through an example, for which we choose the axial anomaly of massless QED, well known

---

[7]Note that although FDF is designed to reproduce FDH results, the FDF scalar is fundamentally different from the ϵ scalar which appears in FDH [45].
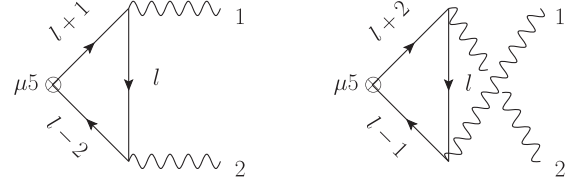
FIG. 1. The two Feynman diagrams for the axial anomaly. The inserted axial current operator is labeled $\mu 5 \otimes$.

for causing inconsistencies if not treated correctly. To calculate the anomaly, we consider the axial current $j^{\mu 5} = \bar\psi \gamma^\mu \gamma^5 \psi$, and the divergence $\partial_\mu j^{\mu 5}$ of its matrix element to create two photons. The matrix element is calculated using the two diagrams in Fig. 1, and is well known (see, e.g., [42,76–79]) to equal

$$= \frac{ie^2}{(4\pi)^2} \mathrm{Tr}\left[\gamma^5 \slashed{l}\, \slashed{\epsilon}^*_1 \slashed{2}\, \slashed{\epsilon}^*_2\right], \qquad (26)$$

where $1, 2 \equiv p_1, p_2$ are the (outgoing) momenta of the two photons with polarization vectors $\epsilon^*_1, \epsilon^*_2$.

To obtain a comparison to chirality flow, we choose a set of polarizations, then use Eqs. (A5) and (A6) to express the polarization vectors and momenta in terms of spinors, obtaining

$$\frac{ie^2}{(4\pi)^2}\mathrm{Tr}[\gamma^5 \slashed{l}\slashed{\epsilon}_{1_L}\slashed{2}\slashed{\epsilon}_{2_R}] = \frac{ie^2}{(4\pi)^2}\frac{2}{\langle r_1 1\rangle[2r_2]}$$
$$\times [-\langle 1r_1\rangle[12]\underbrace{\langle 22\rangle}_{0}[r_2 1] + \underbrace{[11]}_{0}\langle r_1 2\rangle[2r_2]\langle 21\rangle] = 0,$$

$$\frac{ie^2}{(4\pi)^2}\mathrm{Tr}[\gamma^5 \slashed{l}\slashed{\epsilon}_{1_L}\slashed{2}\slashed{\epsilon}_{2_L}] = \frac{ie^2}{(4\pi)^2}\frac{2}{\langle r_1 1\rangle\langle r_2 2\rangle}$$
$$\times [-\langle 1r_1\rangle[12]\langle 2r_2\rangle[21] + \underbrace{[11]}_{0}\langle r_1 2\rangle\underbrace{[22]}_{0}\langle r_2 1\rangle]$$

$$= \frac{2ie^2}{(4\pi)^2}[12]^2, \qquad (27)$$

where we used the explicit representation of γ^5 in the chiral basis to separate the trace into two terms, and the cyclicity of the trace to write everything in terms of spinor inner products. Notice that the axial anomaly vanishes if the photons have opposite helicity.

We now go through the calculation leading up to Eqs. (26) and (27) in chirality flow.[8] It is easiest to set

---

[8]To see this calculation in the pure FDF formalism, see [42].

the polarizations and the reference vectors of the photons at the beginning. We choose ϵ_{1_L} with $r_1 = 2$ and ϵ_{2_R} with $r_2 = 1$. Using the QED vertex, Eq. (8); fermion propagator, Eq. (21); and splitting the trace of γ matrices into two two-component traces, we have

$$i(p_1 + p_2)_\mu \,{}^{\mu 5}\otimes \quad = \frac{2e^2}{\langle 21\rangle [21]} \int \frac{d^d l_{[d]}}{(2\pi)^d} \Bigg\{$$

$$\times \frac{1}{l_{[d]}^2 (l+1)_{[d]}^2 (l-2)_{[d]}^2} \,,$$

$$(28)$$

which is immediately simplified since all terms proportional to μ^2 and parts of the first two chirality-flow diagrams vanish, due to $\langle ii\rangle = [jj] = 0$ and/or due to the Weyl equation, e.g., $\not{2}|2\rangle = 0$ [here, and in the rest of the paper, we use the slash notation to refer to contraction with a Pauli matrix; see Eq. (A5)]. Note how the clever choice of reference vectors helps remove many terms, as at tree level. Although in principle, this is not new to chirality flow, the flow representation makes it obvious.

Next, we swap the arrow directions on all flow lines in the second chirality-flow diagram, and separate the momenta in the $l+1$ and $l-2$ momentum dots of the first chirality-flow diagram to obtain

$$i(p_1 + p_2)_\mu \,{}^{\mu 5}\otimes \quad = \frac{2e^2}{\langle 21\rangle [21]} \int \frac{d^d l_{[d]}}{(2\pi)^d} \Bigg\{$$

$$\times \frac{1}{\left[l_{[d]}^2 (l+1)_{[d]}^2 (l-2)_{[d]}^2\right]} = 0$$

$$(29)$$

where, reading out the inner products, we see that the first two chirality-flow diagrams cancel each other, as do the two last two chirality-flow diagrams. Therefore, in chirality flow, the axial anomaly for opposite-helicity photons can be made to vanish *before* having to do the integration, with —similar to tree level—a significant simplification coming from our choice of reference vectors.

Note that if the terms did not cancel, they would anyway individually vanish after integration. For example, the first chirality-flow diagram can be rewritten as

$$\int \frac{d^d l_{[d]}}{(2\pi)^d} \frac{1}{\left[l_{[d]}^2 (l+1)_{[d]}^2 (l-2)_{[d]}^2\right]} = \langle 21\rangle [12] \qquad (30)$$

$$\times \int \frac{d^d l_{[d]}}{(2\pi)^d} \frac{\langle 2|\bar{l}|1]\langle 2|\bar{l}|1]}{\left[l_{[d]}^2 (l+1)_{[d]}^2 (l-2)_{[d]}^2\right]} \,,$$

which is a rank-two tensor integral. This integral can be solved using standard (d-dimensional) tensor analysis

$$\int \frac{d^d l_{[d]}}{(2\pi)^d} \frac{l^\mu_{[d]} l^\nu_{[d]}}{l^2_{[d]} (l+1)^2_{[d]} (l-2)^2_{[d]}}$$
$$= C_{00} g^{\mu\nu} + C_{11} 1^\mu 1^\nu + C_{22} 2^\mu 2^\nu + C_{12} (1^\mu 2^\nu + 1^\nu 2^\mu), \quad (31)$$

where we used that $\bar{l} \equiv l^\mu_{[4]} \bar{\sigma}_{[4]\mu} = l^\mu_{[d]} \bar{\sigma}_{[4]\mu}$ due to the projective nature of the metric, Eq. (16). However, every coefficient C_{ij} multiplies a vanishing contribution, either due to the Weyl equation, e.g., $C_{11} \langle 2|\bar{\gamma}|1] \langle 2|\bar{\gamma}|1] = 0$, or due to the Fierz identity, $C_{00} \langle 2|\bar{\sigma}^\mu|1] \langle 2|\bar{\sigma}_\mu|1] = 2 C_{00} \langle 22 \rangle [11] = 0$. This exemplifies one of the major advantages of chirality flow for loop diagrams.

If we instead choose photon 2 to be "left chiral" (have positive helicity), i.e., ϵ_{1_L} with $r_1 = 2$ and ϵ_{2_L} with $r_2 = 1$, we get

$$(32)$$

Tensor integrals with three-loop momenta, $I^d_{i_1 i_2 i_3}[l^\mu l^\nu l^\rho]$, can be reduced by using [4]

$$(33)$$

and we can then write the Lorentz structure as spinor products and strings to obtain (after cancellation of some terms)

$$(34)$$

where we used that $l^2_{[d]} = l^2_{[4]} - \mu^2$ from Eq. (24). To solve this, we have to solve three integrals, which, using standard tensor reduction, we write as

$$\int \frac{d^d l_{[d]}}{(2\pi)^d} \frac{l^\mu_{[d]}}{(l+1)^2_{[d]} (l-2)^2_{[d]}} = C^{[0]}_1 1^\mu + C^{[0]}_2 2^\mu,$$

$$\int \frac{d^d l_{[d]}}{(2\pi)^d} \frac{l^\mu_{[d]} l^\nu_{[d]}}{l^2_{[d]} (l+1)^2_{[d]} (l-2)^2_{[d]}} = C_{00} g^{\mu\nu} + C_{11} 1^\mu 1^\nu$$
$$+ C_{22} 2^\mu 2^\nu$$
$$+ C_{12} (1^\mu 2^\nu + 1^\nu 2^\mu),$$

$$\int \frac{d^d l_{[d]}}{(2\pi)^d} \frac{\mu^2}{l^2_{[d]} (l+1)^2_{[d]} (l-2)^2_{[d]}} = C_{[\mu^2]}, \quad (35)$$

such that

$$(36)$$

where it was again obvious due to the Weyl equation that not all tensor coefficients were required. Using Eq. (25) for the integral with μ^2, and calculating the tensor coefficients using [75,80–84] we find

$$C^{[0]}_1 - C^{[0]}_2 + 4 C_{00} + 2 C_{12} \langle 12 \rangle [21] = 0, \quad C_{[\mu^2]} = \frac{1}{2} \frac{i}{(4\pi)^2},$$

$$(37)$$

and therefore we obtain the known result for the anomaly, Eq. (27):
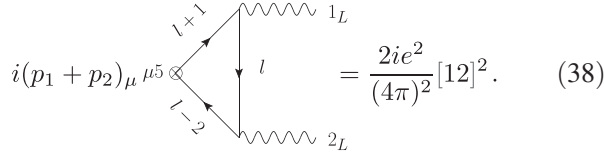
$$i(p_1 + p_2)_\mu \, {}^{\mu 5} \otimes \qquad = \frac{2ie^2}{(4\pi)^2}[12]^2. \qquad (38)$$

This example shows many of the features of chirality flow at one loop. We saw that many terms vanished due to the choice of reference vector, as well as a transparent simplification of the tensor reduction.

Though it was not required in this example, we may also need to take some care with chirality-flow arrows and minus signs at one loop (see the discussion of the fermion self-energy in Sec. IV B). This, along with other details of one-loop chirality-flow calculations, will be discussed below.

A. Reduction of tensor integrals

The method of performing one-loop calculations with chirality flow explored here is traditional in the sense that we do not exploit unitarity-based approaches, but rely on separating the numerator algebra from a tensor integral, which is then decomposed into the various tensor structures, and subsequently reduced to master integrals. The chirality-flow method allows one to use spinor identities and equations of motion directly, such as to directly identify those tensor structures which will not contribute to an amplitude.

In fact the diagrams in the examples above are not ideally suited to chirality flow, as they contain fermion propagators, giving rise to the momentum dots. Instead, the largest amount of simplification comes from internal gauge bosons which (in Feynman gauge) simply give rise to two chirality flows, as exemplified in Eq. (12), or external gauge bosons which [for example for $r_9 = 10^L$ in Eq. (12)] can be chosen to make diagrams vanish. Beyond this, translating gauge bosons to flows opens up for reformulating the four-gluon vertex using Schouten identities, which can give rise to further simplifications as illustrated in [85]. Generally, the flow description allows for identifying vanishing spinor contractions arbitrarily far inside Feynman diagrams, as long as no momentum dots spoil the direct contraction of external (reference) spinors.

As we saw in the axial anomaly above, it is easy to identify which contributions of a tensor integral in chirality flow will vanish. A typical rank-n tensor integral will occur as

$$\langle i_1|\bar{\sigma}_{\mu_1}|j_1] \ldots \langle i_n|\bar{\sigma}_{\mu_n}|j_n] I^d_{d_1 \ldots d_k}[l^{\mu_1} \ldots l^{\mu_n}],$$

$$\langle i_1|\bar{\sigma}_{\mu_1}\sigma_{\mu_2}|j_1\rangle \ldots \langle i_n|\bar{\sigma}_{\mu_n}|j_n] I^d_{d_1 \ldots d_k}[l^{\mu_1} \ldots l^{\mu_n}],$$

$$\langle i_1|\bar{\sigma}_{\mu_1}\sigma_{\mu_2}|j_1\rangle \ldots [i_n|\sigma_{\mu_{n-1}}\bar{\sigma}_{\mu_n}|j_n] I^d_{d_1 \ldots d_k}[l^{\mu_1} \ldots l^{\mu_n}],$$

$$\text{etc.,} \qquad (39)$$

and coefficients will vanish for one of three reasons. Either they will vanish due to the Weyl equation, e.g., $\bar{\jmath}_1|j_1] = 0$; due to massless momenta being contracted with consecutive Pauli matrices, e.g., $\jmath_1\bar{\jmath}_1 = j_1^2 = 0$; or from the Fierz identity contracting two spinor strings with a common spinor, e.g.,

$$\langle i_1|\bar{\sigma}^\mu|j_1][j_1|\sigma_\mu|i_2] = 2\langle i_1 i_2\rangle[j_1 j_1] = 0, \qquad (40)$$

where we define a string of spinors to be a sequence like $\langle i_1|\bar{\sigma}^\mu|j_1]$ which starts and ends with spinors, possibly with (many) Pauli matrices in between.

In general, the number of contributing structures in a tensor integral is dependent on the choice of gauge or spin reference momenta, and, like at tree level, choosing these wisely can significantly reduce the amount of work required to do the calculation.

Additionally, in chirality flow we are sometimes able to reduce the rank of a tensor integral by using equations such as Eq. (33). In [4], we showed how to reduce strings of multiple momentum dots into simpler building blocks, using, e.g.,

$$\cdots = 2l_{[4]} \cdot p_{[4]} \qquad \qquad (41)$$

where the former occurs in diagrams like
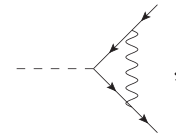
while the latter appears in, e.g., the axial anomaly calculation of the previous section. To use these relations, recall that the momenta on the denominator are d-dimensional, so we have to convert the four-dimensional dot products of Eq. (41) to d-dimensional ones using

$$l^2_{[4]} = l^2_{[d]} + \mu^2,$$

$$2l_{[4]} \cdot p_{[4]} = 2l_{[d]} \cdot p_{[d]} = (l + p)^2_{[d]} - l^2_{[d]} - p^2_{[d]}, \qquad (42)$$

where we used that p is strictly four-dimensional, so $p_{[4]} = p_{[d]}$. For a full set of relations which can reduce

the rank of a tensor integral, see [4]. Reduction methods of tensor integrals along the lines of [80,81] then allow us to directly reduce coefficients of individual tensor structures.

B. Abelian gauge theories

One-loop diagrams in Abelian theories can be separated into two categories, diagrams like the axial anomaly in Sec. IV which have a purely fermionic loop, and diagrams which have a mixture of fermions and bosons in the loop.

For the former case, the procedure is simple: draw the chirality-flow diagram as at tree level [1,2], putting arrows in their natural position, i.e., against the fermion flow. Then perform the integral, making use of the simplifications from Sec. IV A. The rest of this section deals with the second class of loops, those with bosons and fermions, and shows that these can also be handled.

1. Loops with a single fermion line

The simplest example of such a diagram is the self-energy of a massless fermion in the Feynman gauge. There are two diagrams for this process, one in which the fermion emits and reabsorbs the gauge boson (usually just called a photon below for convenience), and another in which it emits and reabsorbs the FDF scalar. However, the FDF-scalar contribution is proportional to $\Gamma^M \Gamma^M = 0$, so we do not need to consider it.

If we consider just the Lorentz structure of the self-energy, and consider only a single chirality, we have, e.g.,

$$(43)$$

for the numerator structure. In the upper chirality-flow diagram, drawn to follow the Feynman diagram, we see that naively applying chirality flow to the diagram leads to either the photon having arrows in the same direction or the momentum-dot not having a continuous flow, both of which are avoided at tree level [1]. As we will see below, this simply introduces a minus sign into equations. In the lower diagram, we see that chirality flow quickly reduces the loop-level Lorentz structure to a simple tree-level chirality structure (i.e., a Lorentz structure which occurs in a tree-level chirality-flow diagram), without having to apply any anticommutation relations.

We now consider the general case of a single massless fermion emitting a virtual photon, possibly emitting more photons, and then reabsorbing the first virtual photon. The simplest version of this is the fermion self-energy, schematically given in Eq. (43).[9] Considering just the Lorentz algebra, we have for example

$$\rightarrow \bar{\tau}^{\nu}\left(\slashed{p}+\slashed{l}\right)\bar{\tau}_{\nu} = -\left(\bar{\slashed{p}}+\bar{\slashed{l}}\right),$$

$$(44)$$

where the Pauli matrices with repeated index are removed using Eq. (A1), and the remaining Lorentz algebra is calculated using Eqs. (A2) and (A3). Note that our normalization of the Pauli matrices in the fermion-photon vertex, Eq. (8), gives the unusual prefactor of one on the right-hand side (which would have read 2 in the case of Dirac matrices or more traditionally normalized Pauli matrices). In chirality flow, Eq. (44) is drawn as

$$(45)$$

If the massless fermion emitted a photon before reabsorption, we instead obtain

$$\rightarrow \bar{\tau}^{\nu}\left(\slashed{p}+\slashed{l}-\slashed{1}\right)\bar{\tau}^{\nu_1}\left(\slashed{p}+\slashed{l}\right)\bar{\tau}_{\nu}+\mu^2\bar{\tau}^{\nu}\tau^{\nu_1}\bar{\tau}_{\nu}$$

$$= -\left(\bar{\slashed{p}}+\bar{\slashed{l}}\right)\tau^{\nu_1}\left(\bar{\slashed{p}}+\bar{\slashed{l}}-\bar{\slashed{1}}\right)-\mu^2\bar{\tau}^{\nu_1},$$

$$(46)$$

using the same method as in Eq. (44) for the Lorentz algebra. Note that we now have a μ^2 term from the fermion propagator, and that in the first line we obtain μ^2 instead of $-\mu^2$ due to the γ^5 matrices in the propagator. In chirality flow, this relation is

---

[9]The full calculation of the FDF (and therefore chirality flow) fermion self-energy in QED, as well as counterterms, are given in [45].

$$(47)$$

where we see that for chirality flow to look like a tree-level structure, we must reverse the order of the momentum dots in the diagram.

In general, for a massless fermion emitting n photons between emission and absorption of the virtual photon, the Lorentz structure will be sums of terms with the following form:

$$= -(\mu^2)^{n-k} \tau^{\nu_{2k+1}} \dots \tau^{\nu_1},$$
$$(48)$$

where k is an integer satisfying $\max\left(0, \frac{n-1}{2}\right) \leq k \leq n$, we suppress the propagator momenta, and the sequence of Pauli matrices always goes $\tau, \tau\bar\tau\tau, \tau\bar\tau\tau\bar\tau\tau$, etc. Note that this relation only holds for an odd number of Pauli matrices, and that, like in Eq. (47), the order of the Pauli matrices on the bottom line of Eq. (48) is reversed. If the fermion in Eq. (48) is massive, then some powers of μ^2 may be replaced by m^2, and the overall sign in this equation is no longer fixed and is calculated using Eq. (21).

The other thing which could happen if the fermion is massive, is that the external fermions could have the same chirality, say left-left. [This may also happen if we for example replace one of the photons $1\dots n$ in diagrams like Eq. (48) with a scalar particle.] In this case, there will be an even number of Pauli matrices between emission and absorption; it is easy to remove the repeated vector index

using Eq. (A1); and the Feynman diagram will have Lorentz structures of the form

$$= m^{2r+1}(\mu^2)^q \, \delta^{\dot\alpha}_{\ \dot\beta} \,\mathrm{Tr}\left(\bar\tau^{\nu_1} \dots \tau^{\nu_{2k}}\right),$$
$$(49)$$

where k, r, and q are non-negative integers satisfying $n/2 \leq k \leq n$, $r = n - k - q \leq n/2$, and $q \leq n/2$, and the overall sign is determined using Eq. (21).

As a simple example of Eq. (49) we consider the diagram from Eq. (47), but for the case of left-left chiralities coming from the replacement of a $\not p$ with a mass

$$+ m\delta^{\dot\alpha}_{\ \dot\beta}\,\mathrm{Tr}\left[\left(\bar{\not p} + \bar{\not l} - \bar{\not 1}\right)\tau^{\nu_1}\right],$$
$$(50)$$

or in chirality flow

$$(51)$$

where the chirality-flow arrows go against the fermion-flow arrows in order to get the correct sign, as in massive chirality flow [2].

While we have given only half of the chiralities explicitly, swapping the chiralities of the fermions in the above examples is trivial, since it is equivalent to swapping all solid lines for dotted ones and vice versa.[10]

---

[10]If the theory is chiral then the chiral couplings must also be exchanged.

2. Loops with two or more fermion lines

We now consider loops with two or more fermion lines. How to set the chirality-flow lines consistently in these examples is analogous to the procedure in [2], and is perhaps easiest understood by an example (we will give a systematic treatment afterward). Consider the following box diagram, redrawn as a chirality-flow diagram:

$$(52)$$

where the chirality-flow lines have chirality-flow arrows opposing fermion-flow arrows, and photons are drawn as double lines which are not yet connected. We note that we cannot connect the photons' flow lines yet, since their arrow directions do not match. To fix this, we use that the chirality-flow lines will always (at least eventually) end with spinors. Labeling the momenta of these end spinors i and j, we can use

$$\langle i|\bar{\tau}^\mu(\slashed{q} - \slashed{l})\bar{\tau}^\nu|j] = [j|\tau^\nu(\bar{\slashed{q}} - \bar{\slashed{l}})\tau^\mu|i\rangle, \qquad (53)$$

an example of Eq. (A4), to swap the chirality-flow arrows on the bottom line, obtaining

$$(54)$$

where we first swapped the arrows, and then connected the photons using the Fierz identity, leading to a completed chirality-flow diagram. Note that we have, for the first time in this paper, a closed chirality-flow string.[11] Such chirality-flow strings are simply traces of Pauli matrices, or equivalently, strings of inner products.

---

[11]This concept is not new to loop calculations. For example, tree-level QCD diagrams also contained traces of two Pauli matrices from the contraction of two momentum dots from gluon vertices.

If the top fermion line of the box diagram is massive, for a given helicity configuration we will also have to calculate chirality-flow diagrams like

$$(55)$$

In this case, we can already use the Fierz identity to join the rightmost photon, obtaining

$$(56)$$

which has two strings of chirality-flow lines, one from the bottom right to the top left (string 1), and the other from the top right to the bottom left (string 2). To connect these two together, we need to use Eq. (A4) to flip the arrows on one string or the other. If we flip it on the string of lines containing the momentum dot, there is an odd number of inner products, so a minus sign will be introduced. Alternatively, we can flip the arrows on string 1 which has two inner products, and therefore will not introduce a minus sign, obtaining

$$(57)$$

Note that the final result is independent of where we swap the arrows.

In a general one-loop Abelian Feynman diagram with multiple fermion lines in the loop, the general procedure to set the arrow directions is:

(1) Draw the chirality-flow lines for each fermion line with chirality flow opposing fermion flow. (Do not

use the Fierz identity to attach fermion lines together yet.)

(2) Choose a photon to be Fierzed first. If needed, use Eq. (A4) to swap the arrow directions of one of the fermion lines containing this photon, and then use the Fierz identity to connect the flow lines. Note that the chirality-flow lines will always, eventually, end in spinors, even if these spinor ends are not explicitly included in the loop calculation, so Eq. (A4) will always hold.

(3) To Fierz further photons, either repeat step 2 with the fermion lines replaced by the strings of chirality-flow lines, or use one of Eqs. (48) or (49), whichever is appropriate.

(4) Repeat step 3 until all photons are replaced with joined chirality-flow lines. This will give a completed one-loop chirality-flow diagram with fully simplified Lorentz structure.

3. General R_ξ gauge

Since the gauge-parameter (in)dependence is an important cross-check of any perturbative calculation, we here comment on the general R_ξ gauge, for which the photon propagator is

$$
\mu\,\wwarrow{p}\,\nu \;=\; -\frac{i}{p_{[4]}^2}\left(g_{[4]}^{\mu\nu} - (1-\xi)\frac{p_{[4]}^\mu p_{[4]}^\nu}{p_{[4]}^2}\right)\,, \quad (58)
$$

in four dimensions. This is straightforwardly translated into chirality flow by recalling that p^μ will always be contracted with a Pauli matrix, thus becoming a momentum dot [see Eq. (11)],

$$
\mu\,\wwarrow{p}\,\nu \;\to\; -\frac{i}{p_{[4]}^2}\left(\text{—}\!\!\text{—} - (1-\xi)\frac{1}{2p_{[4]}^2}\,\text{⟿}^{p\;p}\text{⟿}\right)\,,
$$

$$
\text{or} \quad \to -\frac{i}{p_{[4]}^2}\left(\text{—}\!\!\text{—} - (1-\xi)\frac{1}{2p_{[4]}^2}\,\text{⟿}^{p\;p}\text{⟿}\right)\,. \tag{59}
$$

If the internal photon is part of a loop, Eq. (58) is modified using the -2ϵ-SRs, Eqs. (19) and (20), to also add the propagator of the FDF scalar, and a cross term,

$$
\mu\,\wwarrow{p}\,\nu \;=\; -\frac{i}{p_{[d]}^2}\left(g_{[d_s]}^{\mu\nu} - (1-\xi)\frac{p_{[d]}^\mu p_{[d]}^\nu}{p_{[d]}^2}\right)
$$

$$
= \underbrace{-\frac{i}{p_{[d]}^2}\left(g_{[4]}^{\mu\nu} - (1-\xi)\frac{p_{[4]}^\mu p_{[4]}^\nu}{p_{[d]}^2}\right)}_{4d\text{ photon}}
$$

$$
\underbrace{-\frac{i}{p_{[d]}^2}\left(-i\mu(1-\xi)\frac{Q^M p_{[4]}^\nu + Q^N p_{[4]}^\mu}{p_{[d]}^2}\right)}_{\text{cross term}}
$$

$$
\underbrace{-\frac{i}{p_{[d]}^2}\left(G^{MN} + \mu^2(1-\xi)\frac{Q^M Q^N}{p_{[d]}^2}\right)}_{\text{FDF scalar}}\,, \tag{60}
$$

which will only contribute for loop integrations with an even number of four-dimensional momenta in the numerator. In fact it would be interesting to use Slavnov-Taylor identities to find out, if the cross term can be eliminated in favor of the other structures all together, something we postpone to future work. In any case, the cross term is easy to add using Eq. (11) for the 4D momentum terms.

4. Light cone gauge

While one would typically refrain from using a light cone gauge in full fixed-order calculations, it is interesting to consider this possibility, since the polarization sum of external transverse vector boson polarizations equals the numerator of the propagator in this gauge, justifying its use as "physical gauge." The light cone gauge is thus particularly interesting when we consider cut loops. In four dimensions, the photon propagator in light cone gauge is

$$
\mu\,\wwarrow{p}\,\nu \;=\; -\frac{i}{p_{[4]}^2}\left(g_{[4]}^{\mu\nu} - \frac{p_{[4]}^\mu n_{[4]}^\nu + p_{[4]}^\nu n_{[4]}^\mu}{n_{[4]}\cdot p_{[4]}}\right)\,, \tag{61}
$$

and can once again straightforwardly be written in chirality flow as

$$
\mu\,\wwarrow{p}\,\nu \;\to\; -\frac{i}{p_{[4]}^2}\left(\text{—}\!\!\text{—} \right.
$$

$$
\left. -\frac{\text{⟿}^{n\;p}\text{⟿} + \text{⟿}^{p\;n}\text{⟿}}{2n_{[4]}\cdot p_{[4]}}\right)\,, \tag{62}
$$

or similarly with reversed arrows. As before, if the internal photon is part of a loop, the d dimensional structures have to be kept. Cutting such propagators with the choice of gauge vector advocated in [48], i.e., $p_{[4]}^\mu - p_{[2\epsilon]}^\mu$, gives us a convenient separation of four-dimensional objects and FDF scalars much like for the general R_ξ gauge. However, beyond this more care needs to be taken. In particular, treating the gauge vector directly as we have done in the four-dimensional case, Eq. (61), might only be possible after we have chosen a definite momentum for it. In general, the FDF scalar analog of the gauge vector is not clear at this point. In addition, the tensor decomposition of the loop integrals needs to include the gauge vector as an additional contribution to the possible tensor structures. As it will typically be taken to be one of the external momenta, though, singularities of Gram matrices need to be carefully monitored. Second, we need to regularize the light cone denominators which is conveniently done with the Mandelstam-Leibrandt prescription [86] (see also [26] for a further discussion on how they would be treated in applying unitarity cut methods). While it is not immediately clear that these complications would be outweighed by the transparent and intuitive structure of the propagator numerator we still consider this to be a viable option to explore in future work. It definitely is relevant in the context of using chirality flow for factorizing (loop) amplitudes in preparing applications in resummation along the lines of [4,27].

5. FDF scalars

One key feature of FDF is the appearance of FDF scalars, which have their own Feynman rules (see [48]). In Abelian theories, there are two new rules: the propagator for the FDF scalar just discussed, and the interaction vertex of the FDF-scalar with a fermion

$$\overset{M}{\underset{\longrightarrow}{\big|}} = ie\gamma^5 \Gamma^M = ie\Gamma^M \left(\underset{0}{-\,\text{-}\!\text{-}\!\text{-}\!\blacktriangleleft\text{-}\!\text{-}\!\text{-}} \quad \underset{\longleftarrow}{0} \right),$$

(63)

where the flow rule is the same as any scalar (up to the coupling) and the sign on the left-chiral part coming from γ^5.

Looking ahead to non-Abelian theories, we find that the Feynman rules for FDF scalars only add ingredients we already know how to treat, such as four-dimensional metrics [Eq. (9)] and four-dimensional momenta [Eq. (11)], together with some of the -2ϵ-SRs which will contract to either 0 or ± 1. Therefore, FDF scalars are a noncomplication from the perspective of chirality flow. We also note that counterterms do not introduce any new structure which the chirality-flow formalism would not be able to handle.

C. Non-Abelian gauge theories

To go from loops in an Abelian theory to those in a non-Abelian theory is straightforward in chirality flow. As we will see below, there is essentially nothing new to the non-Abelian case compared to the Abelian case, only more terms to keep track of.

1. QCD

The aim of this section is to explore what chirality-flow structures we obtain in QCD, and argue that we can always consistently set chirality-flow arrows. We will see that all non-Abelian Feynman diagrams have a Lorentz structure which is either composed of the tree-level structures already described in [1,2], or of the same structures as in an Abelian gauge theory like QED, discussed in the previous section.

Compared to Abelian gauge theories like QED, there are two new features in QCD: the addition of ghosts, and the non-Abelian vertices. The ghosts have a scalar propagator and couple to a gluon with a momentum which is easily flowed [see Eq. (11)], so they are not a complication.

The non-Abelian vertices are built from Lorentz structures we have already treated. This can be seen using a simple illustrative example like

(64)

To understand the flow structure of this diagram, we first recall the Lorentz structure of the triple gluon vertex

$$= i\frac{g_s}{\sqrt{2}} if^{a_1 a_2 a_3} \Big(g^{\mu_1 \mu_2}(p_1 - p_2)^{\mu_3}$$
$$+ g^{\mu_2 \mu_3}(p_2 - p_3)^{\mu_1} + g^{\mu_3 \mu_1}(p_3 - p_1)^{\mu_2} \Big),$$

$$\rightarrow i\frac{g_s}{\sqrt{2}} if^{a_1 a_2 a_3} \left(\vcenter{\hbox{}} \right.$$
$$\left. + \vcenter{\hbox{}} + \vcenter{\hbox{}} \right).$$

(65)

Applying this vertex to the loop diagram in Eq. (64), we find (using Feynman gauge and a massless fermion for simplicity)

$$(66)$$

for the Lorentz structure. Here we see that the first and third terms already have tree-level Lorentz structure, while the second term has the "Abelian" Lorentz structure from Eq. (45) (hence the minus sign), multiplied by a disconnected structure.[12] Therefore, all of the Lorentz structures in this QCD diagram are either tree-level structures from [1], or built from the Lorentz structures already encountered in Abelian gauge theories, and setting a consistent arrow direction is straightforward.

This conclusion holds for any general QCD one-loop diagram. This is because the three- and four-gluon vertices, Eqs. (65) and (A8), break up the Lorentz structure into simpler pieces which either break the loop Lorentz structure into a tree-level Lorentz structure, or create loop Lorentz structures of the form of Eqs. (48) and (49). Further, the ghosts and FDF scalars only add 4D metrics and momenta multiplied by -2ϵ-SRs objects, so again break up the Lorentz structure into either trees or structures like Eqs. (48) and (49).

Finally, since the external gluons can have either set of arrow directions without introducing a minus sign, setting arrows is either the same as at tree level, or follows the Abelian case in Sec. IV B.

2. Other non-Abelian theories

Other non-Abelian theories will similarly be easily flowable as long as they contain Feynman rules with 4D objects like scalars, Weyl and Dirac spinors, polarization vectors, momenta, the metric, γ^μ, and γ^5, together with the -2ϵ-SRs. In the Standard Model, the other non-Abelian theory is the electroweak theory, which behaves like QCD but has the addition of massive polarization vectors, chiral vertices, and more (loop-level) scalars.

Chiral vertices and massive polarization vectors were both discussed in [2]. The chiral vertices are most easily understood by drawing the chirality-flow arrow opposing the fermion-flow arrow, giving

---

[12]Recall that the arrow directions of disconnected chirality-flow structures can be set independently [1].

$$\gamma^\mu P_L \to \sqrt{2} \quad \text{} \quad , \quad \gamma^\mu P_R \to \sqrt{2} \quad \text{} \quad ,$$
$$(67)$$

for $P_{R/L} = (1 \pm \gamma^5)/2$. After having made this assignment, all arrow swaps can be done as previously described.

The massive polarization vectors are given in Eq. (A7), with the transverse polarization vectors having the same structure as massless polarization vectors, while the longitudinal polarization vector corresponds to a momentum dot. Therefore, one consequence of longitudinal polarization vectors is that we can obtain closed chirality-flow strings. For example, the axial anomaly with longitudinally-polarized W bosons has the following Lorentz structure:

$$(68)$$

where both terms have closed chirality-flow strings. (The chiral projectors ensure that these are the only two Lorentz structures in the calculation.) These closed flow loops can either be written as sums of spinor products or as traces of Pauli matrices.

Finally, we comment on the fermion self-energy in a theory with a spontaneously broken symmetry like the Standard Model. As shown in Eq. (45), in the Feynman gauge the contribution from a boson of mass m to the self-energy is

$$(69)$$

where we label the generic coupling factors as g^2 and ignore factors of -1, i, and $\sqrt{2}$. Note that it is obvious in chirality flow that this has exactly the same structure as the contribution from a Goldstone boson of mass $m_G = m$
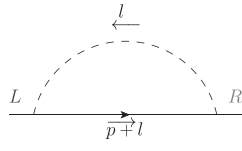
$$\sim (g')^2 \int \frac{d^d l_{[d]}}{(2\pi)^d} \frac{1}{(l^2-m^2)(l+p)^2}, \tag{70}$$

where $g' \neq g$ is the coupling of the Goldstone to the fermion. This type of transparency is one of the nice features of chirality flow at both the tree and one-loop level.

Further, in a general R_ξ gauge, we can use relations such as Eq. (41) to relate the extra terms to the Goldstone contribution. We envisage that the cancellation of gauge-parameter dependence can thus be made more manifest by using chirality flow.

V. CONCLUSION

The chirality-flow formalism has already proven to significantly reduce the amount of work required for calculating tree-level amplitudes, both with pen and paper calculations (where the result often is trivial to obtain) and in computer implementations where the speed gain exceeds 10 for a simple QED test implementation.

While similar algebraic manipulations of amplitudes have been used before the chirality-flow formalism, the graphical algorithm expressed at the level of Feynman rules allows us to transparently employ the simplifications far inside Feynman diagrams in a systematic way. This should also make the formalism suitable for recursive algorithms.

In this paper we have taken the first steps toward exploiting chirality flow beyond tree level. We conclude that many of the simplifications seen at tree level can be retained in the four-dimensional formulation of the 4D helicity scheme. In particular, the Lorentz algebra can be elegantly simplified, and Feynman diagrams can be made to vanish by picking adequate reference vectors for external gauge bosons and massive spinors, as at tree level. We note that while gauge reference vectors bring simplifications also without chirality flow, flowing entire diagrams makes it possible to identify such cancellations even far inside Feynman diagrams.

Beyond this, we find that the tensor reduction procedure is also simplified for one of two reasons, either because we reduce the number of required coefficients in the tensor decomposition, or because we reduce the rank of the tensor integral. The former may happen either directly due to the Weyl equation, or when applying the Fierz identity, while the latter occurs when multiple momentum dots containing the loop momentum are contracted together.

No conceptual problem is preventing the extension of our formalism beyond one loop. However, our current understanding is that four-dimensional regularization schemes beyond one loop are still not strictly proven to be consistent, though there are hints toward their validity beyond one-loop [87]. We expect the main structures discussed in this article, as well as the simplifications and insights they provide, to remain present for calculations beyond one loop, and it is of course highly interesting to also consider other flavors of dimensional regularization tailored to four-dimensional objects, which we will address in the future. Also, note that we did not use any numerators to cancel denominators, such that our formalism will not hit any problem connected to the presence of irreducible numerators beyond one loop. Let us also stress that a fully consistent treatment of regularization will allow us to use chirality flow rules to determine factorized contributions such as splitting functions or soft currents.

APPENDIX: ADDITIONAL CHIRALITY-FLOW RULES

In this section we collect the chirality-flow rules required for this paper which are not stated in the main text. Additional chirality-flow rules can be found in [1,2].

We begin with some algebra relations required to prove Eqs. (44)–(51). The vector indices of the Pauli matrices can be contracted using

$$\tau_\mu^{\dot\alpha\beta}\bar\tau^\mu_{\gamma\dot\eta} = \delta_\gamma^{\ \beta}\delta^{\dot\alpha}_{\ \dot\eta}, \qquad \bar\tau^\mu_{\alpha\dot\beta}\bar\tau_{\mu,\gamma\dot\eta} = \epsilon_{\alpha\gamma}\epsilon_{\dot\beta\dot\eta},$$
$$\tau^{\mu,\dot\alpha\beta}\tau_\mu^{\dot\gamma\eta} = \epsilon^{\dot\alpha\dot\gamma}\epsilon^{\beta\eta}, \tag{A1}$$

while a τ can be turned into a $\bar\tau$ or vice versa using

$$\bar\tau^\mu_{\alpha\dot\beta} = \epsilon_{\alpha\gamma}\epsilon_{\dot\beta\dot\eta}\tau^{\mu,\dot\eta\gamma}, \qquad \tau^{\mu,\dot\alpha\beta} = \epsilon^{\dot\alpha\dot\gamma}\epsilon^{\beta\eta}\bar\tau^\mu_{\eta\dot\gamma}, \tag{A2}$$

where the index positions are crucial, because

$$\epsilon_{\alpha\beta}\epsilon^{\beta\gamma} = \delta_\alpha{}^\gamma, \qquad \epsilon^{\dot\alpha\dot\beta}\epsilon_{\dot\beta\dot\gamma} = \delta^{\dot\alpha}{}_{\dot\gamma},$$
$$\epsilon_{\alpha\beta} = -\epsilon_{\beta\alpha}, \qquad \epsilon_{\dot\beta\dot\gamma} = -\epsilon_{\dot\gamma\dot\beta}. \tag{A3}$$

Next, we recall the equations behind arrow flips. A string of chirality-flow lines can have all of its arrows flipped using one of

$$\langle i|\bar\tau^{\mu_1}\dots\bar\tau^{\mu_{2n+1}}|j] = [j|\tau^{\mu_{2n+1}}\dots\tau^{\mu_1}|i\rangle,$$
$$\langle i|\bar\tau^{\mu_1}\dots\tau^{\mu_{2n}}|j\rangle = -\langle j|\bar\tau^{\mu_{2n}}\dots\tau^{\mu_1}|i\rangle,$$
$$[i|\tau^{\mu_1}\dots\bar\tau^{\mu_{2n}}|j] = -[j|\tau^{\mu_{2n}}\dots\bar\tau^{\mu_1}|i], \tag{A4}$$

where we note that the Pauli matrices stand in a sequence $\tau\bar\tau\tau\dots$ or $\bar\tau\tau\bar\tau\dots$. In practice, when swapping the chirality-flow arrows on a string of flow lines, if the endpoints of the string have the same chirality (line type) then a minus sign is required, while if the endpoints are of opposite chirality (line type) then no minus sign is needed.

In the spinor helicity formalism, for example when converting the axial anomaly from Eqs. (26) to (27), it can be useful to write all objects as (sums of) outer products of spinors. For example, every momentum can be written as

$$\not{p} \equiv p^\mu\sigma_\mu \overset{p_i^2=0}{=} \sum_i |i\rangle\langle i|, \quad \bar{\not{p}} \equiv p^\mu\bar\sigma_\mu \overset{p_i^2=0}{=} \sum_i |i]\langle i|, \tag{A5}$$

where we used that $p = \sum_i p_i$ with $p_i^2 = 0$ to write a massive momentum p as a sum of massless ones [see Eq. (4)], and the massless polarization vectors in Eq. (3) can be written as

$$\not{\epsilon}_L(p_i,r) = \frac{|i]\langle r|}{\langle ri\rangle} \quad \text{or} \quad \bar{\not{\epsilon}}_L(p_i,r) = \frac{|r\rangle[i|}{\langle ri\rangle},$$
$$\not{\epsilon}_R(p_i,r) = \frac{|r]\langle i|}{[ir]} \quad \text{or} \quad \bar{\not{\epsilon}}_R(p_i,r) = \frac{|i\rangle[r|}{[ir]}. \tag{A6}$$

In our discussion of non-Abelian theories, we require the polarization vectors of outgoing massive particles

$$\left(\epsilon_+^\mu(p^\flat,q)\right)^* \longrightarrow \frac{1}{\langle qp^\flat\rangle}$$

or

$$\frac{1}{\langle qp^\flat\rangle}$$

$$\left(\epsilon_-^\mu(p^\flat,q)\right)^* \longrightarrow \frac{1}{[p^\flat q]}$$

or

$$\frac{1}{[p^\flat q]}$$

 $\tag{A7}$

$$\left(\epsilon_0^\mu(p^\flat,q)\right)^* \longrightarrow \frac{1}{m\sqrt{2}}$$

or

$$\frac{1}{m\sqrt{2}}$$

as well as the four-gluon vertex

$$= i\left(\frac{g_s}{\sqrt{2}}\right)^2 \sum_{Z(2,3,4)} if^{a_1a_2b}if^{ba_3a_4}$$
$$\times \left(g^{\mu_1\mu_3}g^{\mu_2\mu_4} - g^{\mu_1\mu_4}g^{\mu_2\mu_3}\right),$$
$$\rightarrow i\left(\frac{g_s}{\sqrt{2}}\right)^2 \sum_{Z(2,3,4)} if^{a_1a_2b}if^{ba_3a_4}$$
$$\times \left(\quad - \quad \right), \tag{A8}$$

where $Z(2,3,4)$ denotes the set of cyclic permutations of the integers 2,3,4, and in both cases the arrow directions which give a continuous flow in a given diagram are chosen.

[1] A. Lifson, C. Reuschle, and M. Sjodahl, Eur. Phys. J. C **80**, 1006 (2020).

[2] J. Alnefjord, A. Lifson, C. Reuschle, and M. Sjodahl, Eur. Phys. J. C **81**, 371 (2021).

[3] A. Lifson, M. Sjodahl, and Z. Wettersten, Eur. Phys. J. C **82**, 535 (2022).

[4] S. Plätzer and M. Sjodahl, arXiv:2204.03258.

[5] P. De Causmaecker, R. Gastmans, W. Troost, and T. T. Wu, Nucl. Phys. **B206**, 53 (1982).

[6] F. A. Berends, R. Kleiss, P. De Causmaecker, R. Gastmans, and T. T. Wu, Phys. Lett. **103B**, 124 (1981).

[7] F. A. Berends, R. Kleiss, P. De Causmaecker, R. Gastmans, W. Troost, and T. T. Wu, Nucl. Phys. **206B**, 61 (1982).

[8] P. De Causmaecker, R. Gastmans, W. Troost, and T. T. Wu, Phys. Lett. **105B**, 215 (1981).

[9] F. A. Berends, R. Kleiss, P. de Causmaecker, R. Gastmans, W. Troost, and T. T. Wu (CALKUL Collaboration), Nucl. Phys. **B239**, 382 (1984).

[10] G. R. Farrar and F. Neri, Phys. Lett. **130B**, 109 (1983); **152B**, 445(A) (1985).

[11] R. Kleiss, Nucl. Phys. **B241**, 61 (1984).

[12] F. A. Berends, P. H. Daverveldt, and R. Kleiss, Nucl. Phys. **B253**, 441 (1985).

[13] J. F. Gunion and Z. Kunszt, Phys. Lett. **159B**, 167 (1985).

[14] J. F. Gunion and Z. Kunszt, Phys. Lett. **161B**, 333 (1985).

[15] R. Kleiss and W. J. Stirling, Nucl. Phys. **B262**, 235 (1985).

[16] K. Hagiwara and D. Zeppenfeld, Nucl. Phys. **B274**, 1 (1986).

[17] R. Kleiss, Z. Phys. C **33**, 433 (1987).

[18] R. Kleiss and W. J. Stirling, Phys. Lett. B **179**, 159 (1986).

[19] Z. Xu, D.-H. Zhang, and L. Chang, Nucl. Phys. **B291**, 392 (1987).

[20] S. Dittmaier, Phys. Rev. D **59**, 016007 (1998).

[21] C. Schwinn and S. Weinzierl, J. High Energy Phys. 05 (2005) 006.

[22] L. J. Dixon, in *QCD and beyond. Proceedings, Theoretical Advanced Study Institute in Elementary Particle Physics, TASI-95, Boulder, USA, 1995* (1996), pp. 539–584, arXiv: hep-ph/9601359.

[23] H. Elvang and Y.-t. Huang, arXiv:1308.1697.

[24] J. R. Forshaw, J. Holguin, and S. Plätzer, J. High Energy Phys. 08 (2019) 145.

[25] M. De Angelis, J. R. Forshaw, and S. Plätzer, Phys. Rev. Lett. **126**, 112001 (2021).

[26] S. Plätzer and I. Ruffa, J. High Energy Phys. 06 (2021) 007.

[27] S. Plätzer, J. High Energy Phys. 07 (2023) 126.

[28] G. 't Hooft and M. Veltman, Nucl. Phys. **B44**, 189 (1972).

[29] P. Breitenlohner and D. Maison, Commun. Math. Phys. **52**, 11 (1977).

[30] D. R. T. Jones and J. P. Leveille, Nucl. Phys. **B206**, 473 (1982); **B222**, 517(E) (1983).

[31] J. G. Korner, D. Kreimer, and K. Schilcher, Z. Phys. C **54**, 503 (1992).

[32] D. Kreimer, arXiv:hep-ph/9401354.

[33] S. A. Larin, Phys. Lett. B **303**, 113 (1993).

[34] T. L. Trueman, Z. Phys. C **69**, 525 (1996).

[35] F. Jegerlehner, Eur. Phys. J. C **18**, 673 (2001).

[36] E.-C. Tsai, arXiv:0905.1479.

[37] E.-C. Tsai, Phys. Rev. D **83**, 025020 (2011).

[38] R. Ferrari, arXiv:1403.4212.

[39] R. Ferrari, Int. J. Theor. Phys. **56**, 691 (2017).

[40] R. Ferrari, arXiv:1605.06929.

[41] A. Viglioni, A. Cherchiglia, A. Vieira, B. Hiller, and M. Sampaio, Phys. Rev. D **94**, 065023 (2016).

[42] C. Gnendiger and A. Signer, Phys. Rev. D **97**, 096006 (2018).

[43] A. Bruque, A. Cherchiglia, and M. Pérez-Victoria, J. High Energy Phys. 08 (2018) 109.

[44] H. Bélusca-Maïto, A. Ilakovac, M. Mađor-Božinović, P. Kühler, and D. Stöckinger, in 16th DESY Workshop on Elementary Particle Physics: Loops and Legs in Quantum Field Theory 2022 (2022), arXiv:2208.02752.

[45] C. Gnendiger *et al.*, Eur. Phys. J. C **77**, 471 (2017).

[46] G. Heinrich, Phys. Rep. **922**, 1 (2021).

[47] C. G. Bollini and J. J. Giambiagi, Nuovo Cimento B **12**, 20 (1972).

[48] R. A. Fazio, P. Mastrolia, E. Mirabella, and W. J. Torres Bobadilla, Eur. Phys. J. C **74**, 3197 (2014).

[49] I. Jack, D. R. T. Jones, and K. L. Roberts, Z. Phys. C **62**, 161 (1994).

[50] I. Jack, D. R. T. Jones, and K. L. Roberts, Z. Phys. C **63**, 151 (1994).

[51] Z. Bern and D. A. Kosower, Nucl. Phys. **B379**, 451 (1992).

[52] Z. Bern, A. De Freitas, and L. J. Dixon, J. High Energy Phys. 03 (2002) 018.

[53] O. A. Battistel, A. L. Mota, and M. C. Nemes, Mod. Phys. Lett. A **13**, 1597 (1998).

[54] A. P. Baeta Scarpelli, M. Sampaio, and M. C. Nemes, Phys. Rev. D **63**, 046004 (2001).

[55] A. P. Baeta Scarpelli, M. Sampaio, B. Hiller, and M. C. Nemes, Phys. Rev. D **64**, 046013 (2001).

[56] S. Catani, T. Gleisberg, F. Krauss, G. Rodrigo, and J.-C. Winter, J. High Energy Phys. 09 (2008) 065.

[57] I. Bierenbaum, S. Catani, P. Draggiotis, and G. Rodrigo, J. High Energy Phys. 10 (2010) 073.

[58] A. L. Cherchiglia, M. Sampaio, and M. C. Nemes, Int. J. Mod. Phys. A **26**, 2591 (2011).

[59] R. Pittau, J. High Energy Phys. 11 (2012) 151.

[60] I. Bierenbaum, S. Buchta, P. Draggiotis, I. Malamos, and G. Rodrigo, J. High Energy Phys. 03 (2013) 025.

[61] A. M. Donati and R. Pittau, J. High Energy Phys. 04 (2013) 167.

[62] A. M. Donati and R. Pittau, Eur. Phys. J. C **74**, 2864 (2014).

[63] R. Pittau, Fortschr. Phys. **63**, 601 (2015).

[64] R. J. Hernandez-Pinto, G. F. R. Sborlini, and G. Rodrigo, J. High Energy Phys. 02 (2016) 044.

[65] B. Page and R. Pittau, J. High Energy Phys. 11 (2015) 183.

[66] G. F. R. Sborlini, F. Driencourt-Mangin, R. Hernandez-Pinto, and G. Rodrigo, J. High Energy Phys. 08 (2016) 160.

[67] G. F. R. Sborlini, F. Driencourt-Mangin, and G. Rodrigo, J. High Energy Phys. 10 (2016) 162.

[68] B. Page and R. Pittau, Eur. Phys. J. C **79**, 361 (2019).

[69] W. J. Torres Bobadilla *et al.*, Eur. Phys. J. C **81**, 250 (2021).

[70] R. Pittau and B. Webber, Eur. Phys. J. C **82**, 55 (2022).

[71] P. Mastrolia, A. Primo, U. Schubert, and W. J. Torres Bobadilla, Phys. Lett. B **753**, 242 (2016).

[72] A. Primo and W. J. Torres Bobadilla, J. High Energy Phys. 04 (2016) 125.

[73] F. R. Anger and V. Sotnikov, arXiv:1803.11127.

[74] Z. Bern and A. G. Morgan, Nucl. Phys. **B467**, 479 (1996).

[75] A. I. Davydychev, Phys. Lett. B **263**, 107 (1991).

[76] S. L. Adler, Phys. Rev. **177**, 2426 (1969).

[77] J. S. Bell and R. Jackiw, Nuovo Cimento A **60**, 47 (1969).

[78] S. L. Adler and W. A. Bardeen, Phys. Rev. **182**, 1517 (1969).

[79] M. E. Peskin and D. V. Schroeder, *An Introduction to Quantum Field Theory* (Addison-Wesley, Reading, USA, 1995).

[80] W. T. Giele and E. W. N. Glover, J. High Energy Phys. 04 (2004) 029.

[81] Simon Plätzer , Oneloop—Reducing one loop integrals with integration by parts (2012).

[82] H. H. Patel, Comput. Phys. Commun. **197**, 276 (2015).

[83] H. H. Patel, Comput. Phys. Commun. **218**, 66 (2017).

[84] V. Shtabovenko, Comput. Phys. Commun. **218**, 48 (2017).

[85] E. Boman, A. Lifson, M. Sjodahl, A. Warnerbring, and Z. Wettersten, J. High Energy Phys. 02 (2024) 005.

[86] G. Leibbrandt, Noncovariant gauges (World Scientific, Singapore, 1994).

[87] A. Broggio, C. Gnendiger, A. Signer, D. Stöckinger, and A. Visconti, J. High Energy Phys. 01 (2016) 078.